86 GHz VLBI Survey of Ultra Compact Radio Emission in Active Galactic Nuclei

© **D. G. Nair**[1], **A. P. Lobanov**[1,2], **T. P. Krichbaum**[1], **E. Ros**[1,3,4], **J. A. Zensus**[1]

[1]Max-Planck-Institut für Radioastronomie, Bonn, Germany
[2]Institut für Experimentalphysik, Universität Hamburg, Germany
[3] Departament d'Astronomia i Astrofísica, Universitat de València, Spain
[4]Observatori Astronòmic, Universitat de València, Spain

Very Long Baseline Interferometry (VLBI) Observations at 86 GHz reach a resolution of about 50 μas and sample the scales as small as $10^3 - 10^4$ Schwarzschild radii of the central black hole in Active Galactic Nuclei (AGN), uncovering the jet regions where acceleration and collimation of the relativistic flow takes place. We present the results from a large global VLBI survey of 162 ultra-compact radio sources at 86 GHz conducted in 2010–2011. All the sources were detected and imaged; increasing by a factor of ~ 2 the total number of AGN so far imaged with VLBI at 86 GHz. The survey data attained a baseline sensitivity of 0.1 Jy and a typical image sensitivity of 5 mJy/beam.

We have used Gaussian model fitting to represent the structure of the observed sources and to estimate the flux densities and sizes of the core and jet components. The model fitting yields estimates of the brightness temperature ($T_{\rm b}$) of the compact VLBI (base) of the jet and inner jet components of AGN, taking into account the resolution limits of the data at 3 mm. We have applied a basic population model with a single value of intrinsic brightness temperature, T_0, in order to reproduce the observed distribution of $T_{\rm b}$. The modelling yields $T_0 \sim 1 - 7 \times 10^{11}$ K in the VLBI cores and $T_0 \leq 5 \times 10^{10}$ K in the jets. This finding indicates that the VLBI cores reflect the inverse-Compton limit on brightness temperature, while the properties of the inner jets can be described by the equipartition between the particle and magnetic field energy. We also find a correlation between the brightness temperatures obtained from the model fits with estimates of the brightness temperature limits made directly from the visibility data. For objects with sufficient structural detail detected, we investigated the effect of adiabatic energy losses on the evolution of brightness temperature along the jet.

Keywords: VLBI, Active Galaxies, Jets, Radio continuum, Millimetre surveys, Brightness temperature.

1 Introduction

VLBI observations at 86 GHz (wavelength of 3.4 mm) enable detailed studies of compact radio sources at $\sim 40 - 100$ μas resolution. Synchrotron radiation becomes optically thin at millimetre wavelengths; making it possible to look deeper into the core and inner jets of AGN which are invisible at centimetre and longer wavelengths due to self absorption or free-free absorption by the torus. The high-resolution studies of complete (or nearly complete) samples enable investigations of the physical conditions in the region where jets are launched (e. g. [3], [5]). To date, five 86 GHz VLBI surveys have been conducted (see [1], [8], [10], [12], [15] and Table 1), with the total number of objects imaged reaching just over a hundred. Previous studies (e. g. [8],[10]) indicate that brightness temperatures measured at 86 GHz are systematically lower than that of low frequencies and $\nu_{\rm break}$ can be as low as 20 GHz. If T_0 starts to become smaller in the mm-bands, there may be only a few sources suitable for VLBI at 147 GHz, 215 GHz and higher frequencies. This finding needs to be confirmed by observations of a statistically viable sample at 86 GHz. Also changes of brightness temperature T_0 in the compact jets with frequency can be used to distinguish between the emission coming from accelerating or decelerating plasma and from electron–positron or electron–proton plasma. In view of all these arguments, we have undertaken a dedicated 86 GHz ($\sim$ 3mm) VLBI survey of a larger sample of extragalactic radio sources in 2010–2011 using the Global Millimetre VLBI Array (GMVA). In the following, we present the survey observations and discuss results from the initial analysis of the data.

2 Observations

The survey targeted 162 unique sources, selected from the MOJAVE complete sample ([9]) and the 22 GHz VERA Galactic plane survey ([14]), using the following selection criteria: *a)* correlated flux density, $S_{\rm c} \geq 0.5$ Jy on long baselines ($\geq 400\,{\rm M}\lambda$); *b)* compactness at longest spacings, $S_{\rm c}/S_{\rm VLBA} \geq 0.4$ where $S_{\rm VLBA}$ is the 15 GHz total clean flux density; *c)* declination $\delta \geq -20°$. The observations have been made over the total of 6 days (144 hours), scheduled within three separate GMVA sessions in October 2010, May 2011 and October 2011; with 3–4 scans of 6–7 minutes duration on each source in a snapshot mode with the participation of 14 telescopes (8 VLBA stations and 6 European antennas at Efflesberg, Onsala, Pico Velata, Plateau de Bure, Yebes and Metasähovi). The data were recorded with a total bandwidth of 128 MHz at a recording rate of 512 Mb/s with 2-bit sampling for all the epochs and correlated at the DiFX correlator of the MPIfR in Bonn. The post-processing of the data comprising the detection of interference fringes and the a priori amplitude and phase calibration was done in AIPS. The self-calibration and imaging was done using the Difmap software package.

Table 1

VLBI surveys at 86 GHz

Surveys (1)	$N_{\rm ant}$ (2)	$B_{\rm rec}$ (3)	ΔS (4)	$\Delta I_{\rm m}$ (5)	$D_{\rm img}$ (6)	$N_{\rm obs}$ (7)	$N_{\rm det}$ (8)	$N_{\rm img}$ (9)
1	3	112	~ 0.5	...	...	51	12	...
2	2–5	112/224	~ 0.7	...	...	79	14	...
3	6–9	128	~ 0.5	~ 30	70	68	16	12
4	3–5	224	~ 0.4	~ 20	100	28	26	14
5	12	256	~ 0.3	10	200	127	121	109
This survey	13–14	512	~ 0.1	~ 5	> 400	*162*	*162*	*162*

Columns: 1 — Previous 3 mm VLBI survey's references [1],[12],[15],[10] and [8] respectively; 2 — number of participating antennas; 3 — recording bit rate [Mbps]; 4 — average baseline sensitivity [Jy]; 5 — average image sensitivity [mJy/beam]; 6 — typical dynamic range of images; 7 — number of objects observed; 8 — number of objects detected; 9 — number of objects imaged.

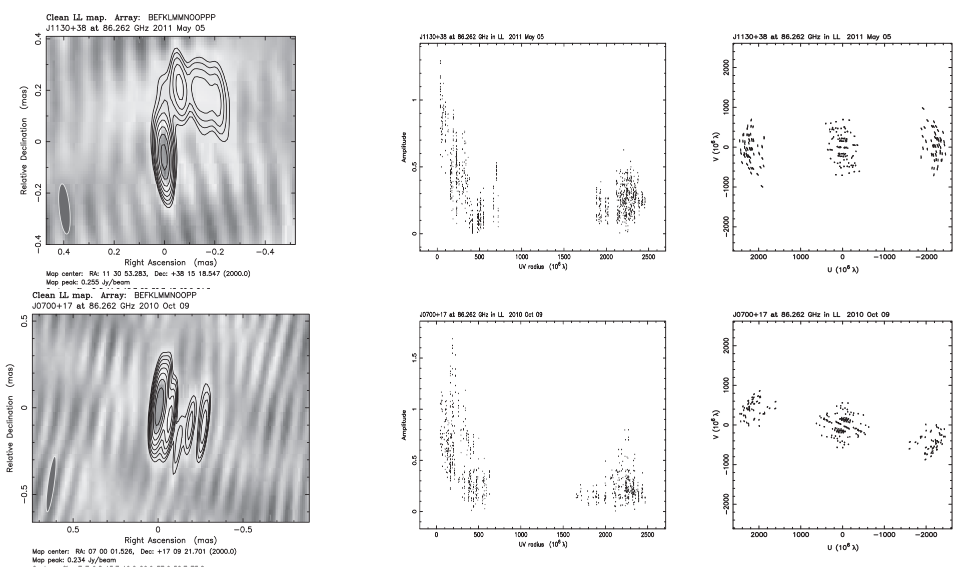

Fig. 1. 3 mm map of J1130+3815 (May 2011 — *top, left*) and J0700+1709 (Oct 2010 — *bottom, left*). Image is convolved with the natural beam. The contour lines start at 3 times the rms noise level. The lowest contour is at 8 mJy and 7 mJy respectively. The visibility amplitude (Jy) vs UV radius ($10^6\,\lambda$) and the uv coverage ($10^6\,\lambda$) for the respective sources is shown on top, right and bottom, right.

For the source J1130+3815, the peak flux density is 0.26 Jy/beam, with a beam size of 0.20×0.04 mas. The brightness temperature of the core component is $(1.54 \pm 0.47) \times 10^{11}$ K.

For the source J0700+1709, the peak flux density is 0.23 Jy/beam, with a beam size of 0.32×0.04 mas. The brightness temperature of the core component is $(1.92 \pm 0.60) \times 10^{11}$ K

3 Results

3.1 3 mm imaging and source modelling

We have detected all of the 174 sources observed and made hybrid CLEAN maps of them with a typical image sensitivity of ~ 5 mJy/beam and a baseline sensitivity of 0.1 Jy increasing the database of sources ever imaged at 86 GHz almost by a factor of 2. The physical parameters of the sources like flux density, size, etc. were derived using Gaussian model fitting the visibilities. The model fitting results showed that about 80 % of the model fit components were resolved. To illustrate our results, we present images of two weak target sources in the survey — J1130+3815 and J0700+1709 in Fig. 1. J1130+3815 is a quasar at a redshift of $z = 1.7$ and its 3 mm image shows one jet feature extending along P.A$\sim 180^\circ$ at a distance of 0.13 mas. J0700+1709 is an unidentified radio source and its 3 mm image shows one jet feature extending along P.A$\sim$167°. These images illustrate well the successful reconstruction of the source structure using snapshot GMVA observations.

3.2 Population modelling for the brightness temperature T_b

We combined the 3 mm data from [8] with the data from this survey and applied a model for the brightness temperature distribution derived from the Gaussian model fitting under the assumption that the jets are randomly oriented in space and the jets have the same Lorentz factor and the same spectral index and the same intrinsic brightness temperature T_0. For such a population of radio sources, the probability to find a radio source with the brightness temperature T_b is proportional to

$$p(T_b) \propto \left[\frac{2\gamma_j \left(T_b/T_0\right)^{\epsilon} - \left(T_b/T_0\right)^{2\epsilon} - 1}{\gamma_j^2 - 1} \right]^{\frac{1}{2}} \tag{1}$$

according to [10]. As depicted in Fig. 2, when the observed T_b from this survey are compared with the theoretical model according to Eqn. 1, the resulting intrinsic brightness temperature for cores lies in the range of $T_0 \sim (1-7) \times 10^{11}$ K and for jet components, it is $T_0 \leq 5 \times 10^{10}$ K. Thus the observed T_b is in a range close to the inverse Compton limit (of $\sim 5 \times 10^{11}$ K) [6],

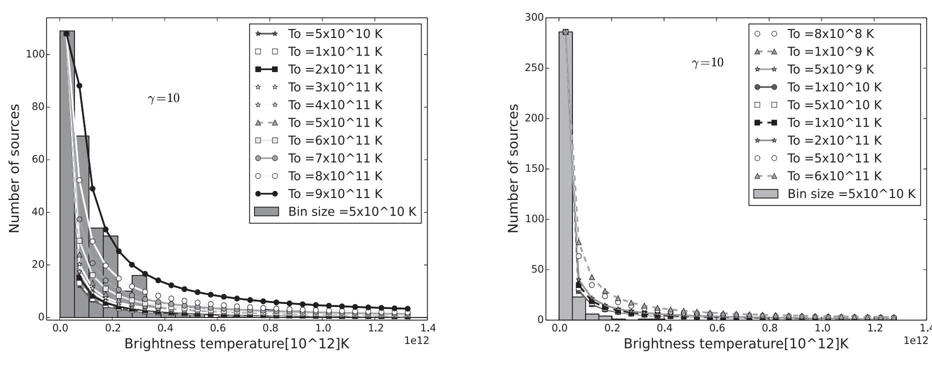

Fig. 2. Distribution of the brightness temperatures, T_b measured in the core (*left*) and jet components (*right*). The curved lines on the plot depict the theoretical distribution of T_b according to Eqn. 1 [10]

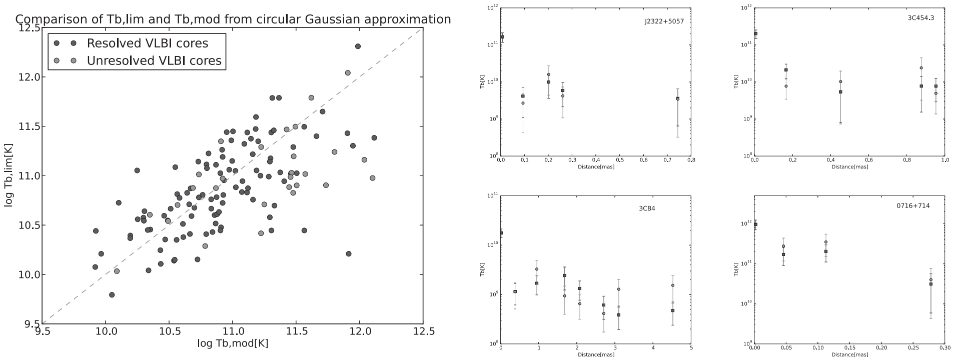

Fig. 3. *Left:* Correlation of $T_{\rm b}$ measured from circular Gaussian approximation of source structure from the 3 mm maps ($T_{\rm b,mod}$) and $T_{\rm b}$ estimated from the theoretical calculation from the direct interferometric visibilities ($T_{\rm b,lim}$). *Right:* Evolution of the brightness temperature along the jet of four sources — J2322+5037, 3C 454.3, 3C 84 and 0716+714 from this survey. Blue squares and red circles represent the measured $T_{\rm b}$ from this survey and theoretically predicted $T_{\rm b}$ by ([8],[10]) respectively if the jets expand adiabatically. The initial brightness temperature in each jet is assumed to be same as that measured in the VLBI core

beyond which the inverse Compton effect causes rapid electron energy losses and extinguishes the synchrotron radiation and T_0 of jet components is in agreement with the equipartition limit $\sim 5 \times 10^{10}$ K [16].

3.3 Brightness temperature limits

We measured the upper limits on brightness temperature ($T_{\rm b,lim}$) made directly from the visibility data as discussed in [11]. The interferometric visibility is expressed as $V = V_{\rm q} e^{-i\phi_{\rm q}}$ described by its amplitude $V_{\rm q}$ and phase $\phi_{\rm q}$. From the angular extent, $T_{\rm b}$ can be calculated by applying the Rayleigh-Jeans limit to the Planck formula, and $T_{\rm b}$ is formulated as

$$T_{\rm b,lim} = \frac{\pi B^2}{2k}(V_q + \sigma_q) \ln \frac{V_q + \sigma_q}{V_q} \tag{2}$$

For each object, the $T_{\rm b,lim}$ is estimated from the 86 GHz data at uv-radii $\geq 0.9 B_{\rm max}$ using Eqn.(2), where $B_{\rm max}$ is the longest baseline distance in the data, in order to restrict the visibility information to the most compact structures. We found that the estimated $T_{\rm b,lim}$ are essentially equal to $T_{\rm b,mod}$ obtained from Gaussian model fitting method which is shown in Fig. 3 (left). Thus, these two methods of core and jet brightness temperature measurements can be used for obtaining brightness temperature from 3 mm VLBI data, giving coherent results.

4 Conclusion

We have presented results from a large global 86 GHz VLBI Survey of compact radio sources using a global millimetre VLBI array. We analysed the T_b distribution in the sample using a basic population model. A compilation of this survey's T_b measurements with that made with ground VLBI at lower frequencies like 2 GHz, 8 GHz, 15 GHz (e. g. [7], [14]) and conversion of frequency to linear scales in the jet using radio luminosity and jet parameters will help to study the evolution of T_0 with frequency, $T_0(\nu)$, and $T_0(r)$, along the jet. This can be used to constrain the bulk Lorentz factor and the intrinsic brightness temperature of the jet plasma, using different types of population models of relativistic jets (e. g. [5]). This will help us to distinguishing between the acceleration and deceleration scenario for the flow as discussed in [13] and to test several alternative acceleration scenarios including acceleration by pressure gradients [2], tangled magnetic field [4] and the MHD acceleration model of Vlahakis and Königl [17].

References

1. *Beasley A. J., Dhawan V., Doeleman S., Philips R. B.* CMVA Observations of Compact AGNs // Proceedings of Millimeter-VLBI Science Workshop. — 1997. — P. 53.
2. *Bodo G., Ferrari A., Massaglia S., Tsinganos K.* Acceleration and thermal instabilities in the jets of SS 433 // Astronomy & Astrophysics — 1985. — Vol. 149. — P. 246–252.
3. *Cohen M. H., Lister M. L., Homan D. C., et al.* Relativistic Beaming and the Intrinsic Properties of Extragalactic Radio Jets // Astrophysical Journal. — 2007. — Vol. 658. — P. 232–244.
4. *Heinz S., Begelman M. C.* Jet Acceleration by Tangled Magnetic Fields // Astrophysical Journal. — 2000. — Vol. 535. — P. 104–117.
5. *Homan D. C., Kovalev Y. Y., Lister M. L., et al.* Intrinsic Brightness Temperatures of AGN Jets // Astrophysical Journal. — 2006. — Vol. 642. — P. L115–L118.
6. *Kellermann K. I., Pauliny -Toth I. I. K.* The Spectra of opaque radio sources // Astrophysical Journal. — 1969. — Vol. 155. — P. L71.
7. *Kovalev Y. Y., Kellermann K. I., Lister M. L., et al.* Sub-Milliarcsecond Imaging of Quasars and Active Galactic Nuclei. IV. Fine-Scale Structure // Astronomical Journal. — 2005. — Vol. 130. — P. 2473–2505.
8. *Lee S. S., Lobanov A. P., Krichbaum T. P., et al.* A Global 86 GHz VLBI Survey of Compact Radio Sources // Astronomical Journal. — 2008. — Vol. 136. — P. 159–180.
9. *Lister M. L., Homan D. C.* MOJAVE: Monitoring of Jets in AGN with VLBA Experiments — I. First-Epoch 15 GHz Linear Polarization Images // Astronomical Journal. — 2005. — Vol. 130. — P. 1389–1417.

10. *Lobanov A. P., Krichbaum T. P., Graham D. A., et al.* 86 GHz VLBI survey of compact radio sources // Astronomy & Astrophysics. — 2000. — Vol. 364. — P. 391.
11. *Lobanov A.* Brightness temperature constraints from interferometric visibilities // Astronomy & Astrophysics. — 2015. — Vol. 574. — P. A84.
12. *Lonsdale C, J., Doelman S. S., Philips R. B.* A 3 Millimeter VLBI Continuum Source Survey // Astronomical Journal. — 1998. — Vol. 116. — P. 8.
13. *Marscher A. P.* Probes of the inner jets of blazars // Proceedings of the National Academy of Science. — 1995. — Vol. 92. — P. 11439–11441.
14. *Petrov L., et al.* VERA 22 GHz fringe search survey // Astronomical Journal — 2007. — Vol. 133. — P. 2487–2494.
15. *Rantakyro F. T., Baath L. B., Backer D. C., et al.* 50 μas resolution VLBI images of AGN's at λ3 mm // Astronomy and Astrophysics Supplement Series — 1998. — Vol. 131. — P. 451–467.
16. *Readhead A. C. S.* Equipartition brightness temperature and the inverse Compton catastrophe // Astrophysical Journal. — 1994. — Vol. 426. — P. 51–59.
17. *Vlahakis N., Königl A.* Magnetic Driving of Relativistic Outflows in Active Galactic Nuclei. I. Interpretation of Parsec-Scale Accelerations // Astronomical Journal — 2004. — Vol. 605. — P. 656–661.